

Pseudogap and doping-dependent magnetic properties of $\text{La}_{2-x}\text{Sr}_x\text{Cu}_{1-y}\text{Zn}_y\text{O}_4$

R. S. Islam,^{1,2} J. R. Cooper,¹ J. W. Loram,¹ and S. H. Naqib^{1,2,*}

¹*Department of Physics, University of Cambridge, J. J. Thomson Avenue, Cambridge CB3 0HE, United Kingdom*

²*Department of Physics, University of Rajshahi, Raj 6205, Bangladesh*

(Received 2 October 2009; revised manuscript received 30 December 2009; published 17 February 2010)

The effects of planar hole content p ($=x$) on the static magnetic susceptibility $\chi(T)$ of polycrystalline $\text{La}_{2-x}\text{Sr}_x\text{Cu}_{1-y}\text{Zn}_y\text{O}_4$ compounds were investigated over a wide range of Sr (x) and Zn (y) contents. The Curie-like magnetic behavior caused by Zn was found to depend strongly on the hole content. The apparent magnetic moment induced by Zn was larger in underdoped $\text{La}_{2-x}\text{Sr}_x\text{Cu}_{1-y}\text{Zn}_y\text{O}_4$, decreased quite sharply around $p \approx 0.19$, and did not change much for further overdoping. This is interpreted in terms of the effect of the pseudogap on the Zn-induced magnetic behavior, as there is growing evidence that the pseudogap vanishes quite abruptly at $p \approx 0.19$. From a detailed analysis of $\chi(T)$ data the Zn-induced magnetic contribution was found to be rather complex and showed non-Curie-like features over a wide range of temperature. For the underdoped samples the low-energy Curie-like excitations are accompanied by a substantial loss of spin spectral weight at around the pseudogap energy. This accounts for the anomalously large “dilution” term in the susceptibility of underdoped samples. This effect is absent in samples with $p \geq 0.19$. The observed behavior was scrutinized in terms of two scenarios: (a) that of independent localized moments and (b) low-energy states associated with each Zn atom. Our study points toward the latter scenario and may suggest that there is a redistribution of quasiparticle spectral weight due to Zn substitution, the features of which are greatly influenced by the presence and magnitude of the pseudogap.

DOI: [10.1103/PhysRevB.81.054511](https://doi.org/10.1103/PhysRevB.81.054511)

PACS number(s): 74.72.-h, 74.25.Ha, 74.25.Dw, 74.62.Dh

I. INTRODUCTION

Cuprate superconductivity arises from strongly interacting charge carriers in the CuO_2 planes. Substituting a single impurity for a copper atom perturbs the surrounding electronic environment and can therefore be used as a probe for understanding the physics of high-temperature superconductors. Experiments on Zn-substituted cuprates provide valuable information on the electronic properties of the host materials, in both the normal and the superconducting (SC) states. Zn^{2+} is a nonmagnetic ion owing to its $3d^{10}$ (spin $s=0$) electronic configuration and is a very strong destroyer of d -wave superconductivity. It has been shown in early years¹ that Zn causes a rapid suppression of T_c , ~ -10 K/% Zn in the CuO_2 plane. Zn is believed to act as a unitary scatterer^{2,3} in suppressing the superconductivity of the host material, without substantially altering the planar hole concentration p .⁴ Electron-spin⁵ and nuclear-magnetic-resonance^{6,7} experiments have indicated that nonmagnetic Zn gives rise to a local magnetic moment-like feature on the four nearest-neighbor Cu sites in the CuO_2 planes. This apparent magnetic behavior is also evident from the appearance of a “Curie-like” term in the bulk magnetic susceptibility of the Zn-doped samples.^{3,8-10} It has been proposed³ that this effect arises from the local suppression of short-range antiferromagnetic (AF) correlations as a result of replacing ($s=1/2$) Cu^{2+} with ($s=0$) Zn^{2+} . Scanning tunneling microscopy experiments on Zn-substituted $\text{Bi}_2\text{Sr}_2\text{CaCu}_2\text{O}_{8+\delta}$ single crystals¹¹ found intense low-energy quasiparticle (QP) scattering resonances at the Zn sites, coincident with the strong suppression of superconductivity within ~ 15 Å of the scattering sites. Complementary results were obtained earlier by Loram *et al.* from their specific-heat measurements,¹² namely, a strong increase in the low-temperature ($T \rightarrow 0$ K)

electronic specific-heat coefficient $\gamma(0)$ with Zn. This implies that Zn is a strong pair breaker that induces a significant residual density of states (DOS) near the Fermi level in the superconducting state. There are also strong arguments in favor of a transfer of spectral weight from high energy to low energy in Zn-substituted compounds¹³ that are supported by some inelastic neutron-scattering experiments.¹⁴ This is interesting because it opens up the possibility of an alternative scenario for explaining the magnetic properties of Zn-doped cuprates, in terms of low-energy states affecting the spin susceptibility, involving a redistribution of QP spectral weight rather than the formation of independent localized magnetic moments. A detailed investigation is still lacking.

In this paper, we report some systematic studies of the effects of planar hole content on the static magnetic susceptibility $\chi(T)$ of $\text{La}_{2-x}\text{Sr}_x\text{Cu}_{1-y}\text{Zn}_y\text{O}_4$ (Zn-LSCO) sintered samples over a wide range of Sr (x) and Zn (y) contents. From the analysis of the $\chi(T)$ data, we have found the Zn-induced Curie-like increase in magnetic susceptibility to be strongly dependent on the hole content and to correlate closely with the presence of the pseudogap (PG). The effect of Zn was also found to be strongly T dependent; however, the behavior does not follow a simple Curie-Weiss (CW) T dependence over the whole temperature range. Instead the temperature dependence is rather complex and we argue that the localized moment scenario, even when supplemented by the Kondo effect, does not offer a complete explanation. Our analysis shows that the more likely scenario is a Zn-induced redistribution of QP spectral weight in this correlated-electron host compound. This redistribution depends strongly on the existence and size of the PG.

II. EXPERIMENTAL DETAILS AND RESULTS

Polycrystalline single-phase sintered samples of $\text{La}_{2-x}\text{Sr}_x\text{Cu}_{1-y}\text{Zn}_y\text{O}_4$ were synthesized by standard solid-state

reaction methods using high-purity (>99.99%) starting materials. Samples were characterized by measurements of x-ray powder diffraction, room-temperature thermopower, and ac susceptibility. Details of sample preparation and characterization can be found elsewhere.¹⁵ $\chi(T)$ measurements were made using a model 1822 Quantum Design superconducting quantum interference device (SQUID) magnetometer. During the measurement the sample was mounted between two quartz tubes of similar dimensions that were attached to the sample rod. The tubes were properly cleaned before each measurement to avoid contamination by any magnetic particles. Data were collected following a predefined sequence, usually in the range of 5–400 K, and for different values of the field so as to check the linear field dependence. A scan length of 6 cm was used. The background signal was due to the absence of quartz at the position of the sample and varied linearly with the separation between the two quartz tubes up to a separation of approximately 6 mm, the length of the samples. Hence, the shape of the SQUID response curve was the same for the sample and for the empty sample holder. This meant that the magnetic moment of the quartz tubes could be subtracted from the data to obtain the magnetic moment of the sample, from which the susceptibility was then obtained. We have investigated five Sr concentrations: two underdoped (UD), 9% and 15% Sr, and three overdoped (OD), 19%, 22%, and 27% Sr. For each Sr content we have measured six Zn contents (0%, 0.5%, 1.0%, 1.5%, 2.0%, and 2.4% Zn) chosen to be within the solubility limit. We attribute anomalous susceptibility data at around 60 K for some of the samples to the presence of absorbed oxygen.

The $\chi(T)$ data are shown in Fig. 1 and are also available electronically.¹⁶ The $\chi(T)$ plots show that (i) a Curie-like term appears at low temperature and that this increases with Zn concentration, (ii) this Curie-like term decreases with increasing Sr content (i.e., with increasing hole doping), and (iii) for the samples with $x > 0.19$, this term is similar in magnitude to that for $x = 0.19$. Therefore, it is apparent that the Zn-induced increase in $\chi(T)$ is larger for UD $\text{La}_{2-x}\text{Sr}_x\text{Cu}_{1-y}\text{Zn}_y\text{O}_4$.

III. DATA ANALYSIS

In the present study we wish to determine the added contribution $\chi_{\text{Zn}}(T)$ due to Zn substitution. Since the host susceptibility in these materials is strongly temperature and Sr doping dependent, we can anticipate significant systematic errors for any given sample due to errors in the Sr content. Therefore, to avoid placing undue weight on the Zn-free sample, we apply a linear fit at each experimental temperature T of the form

$$\chi(T) = a_0(T) + a_1(T)y, \quad (1)$$

where y is the Zn content in at. % and $a_0(T)$ and $a_1(T)$ are the coefficients determined from least-squares fits to the $\chi(T)$ data for a given value of Sr concentration (x). Evidently $a_0(T)$ gives the fitted contribution from the Zn-free sample ($y=0$) and $a_1(T)$ is the increment per % Zn. The justification for using a linear fit comes from the experimental data but is

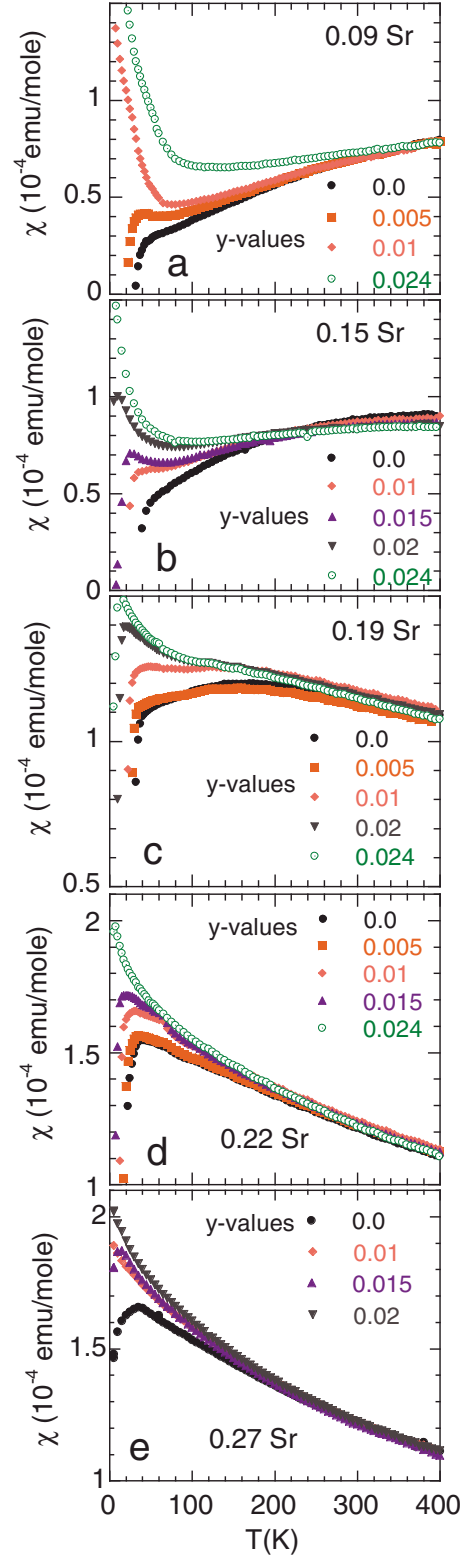


FIG. 1. (Color online) $\chi(T)$ data for $\text{La}_{2-x}\text{Sr}_x\text{Cu}_{1-y}\text{Zn}_y\text{O}_4$ compounds. The Sr (x) and Zn (y) contents are shown. The data are also available electronically (Ref. 16).

expected on general grounds (above the superconducting region) for the low levels of substitution used, up to 2.4% Zn/Cu. In Fig. 2 we show $\chi(T)$ at several different fixed temperatures T_0 , versus Zn content (y) for 15% Sr-doped

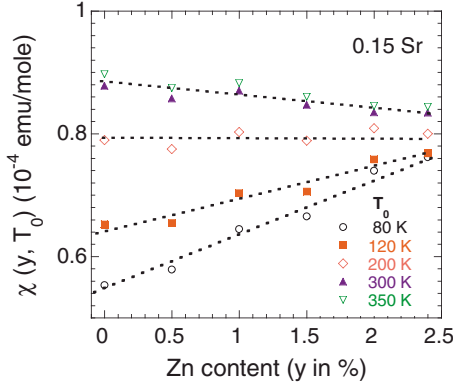


FIG. 2. (Color online) Representative plots of χ vs Zn content (y) at fixed temperatures (T_0) for $\text{La}_{1.85}\text{Sr}_{0.15}\text{Cu}_{1-y}\text{Zn}_y\text{O}_4$. Values of T_0 are shown. Dashed straight lines show linear fits.

LSCO, and this clearly shows the validity of the linear approximation. The results of least-squares fits $\chi_{fit}(T)$ are shown in Fig. 3 where the lower-temperature limit of 50 K has been chosen to avoid the region of significant diamagnetic SC fluctuations. This is easily recognized as the temperature below which the variance and residuals sharply increase. Comparing $\chi_{fit}(T)$ with the raw data in Fig. 1 confirms the quality of the fits. We have marked a crossover temperature T_{cs} in Figs. 3(a) and 3(b) where the $\chi(T, y)$ plots cross each other. Such a feature is absent for the OD compounds. We have also analyzed the error $\Delta\chi(T) = [\chi(T) - \chi_{fit}(T)]$ for the respective compounds. It can be seen from Fig. 4 that for most of the compounds $\Delta\chi(T)$ is less than 2% of the experimental $\chi(T)$ at 400 K. From the T dependences of $\Delta\chi(T)$ we conclude that the systematic errors result mainly from small differences in Sr content at the level of $\Delta x \sim \pm 0.5\%$ Sr.

The coefficient a_0 , representing the fitted values for the Zn-free samples, is shown in Fig. 5(a). The absence of a pseudogap for $p > 0.19$ is evident from this figure. From previous analyses of magnetic susceptibility and specific-heat data^{15,17} we have extracted the PG energy scale T^* , in degrees K, for the LSCO compounds. $T^* = 500$ K for $p = 0.09$ and $T^* = 290$ K for $p = 0.15$.^{15,17} These values correspond approximately to the temperature of the shoulder in χ . Next, the T dependence of the coefficient a_1 is plotted in Fig. 5(b) for different values of Sr content, and it shows the change in magnetic susceptibility per % Zn. $a_1(T)$ shows a Curie-like increase at low temperatures for all samples, with a magnitude that decreases strongly with hole doping. For $p > 0.19$ the Curie-like term is small and almost p independent.

IV. DISCUSSION

In this section we first discuss our data in terms of a conventional local moment analysis. This leads to inconsistencies which are resolved by the entirely model-independent analysis which follows. We finally discuss several possible interpretations of our results.

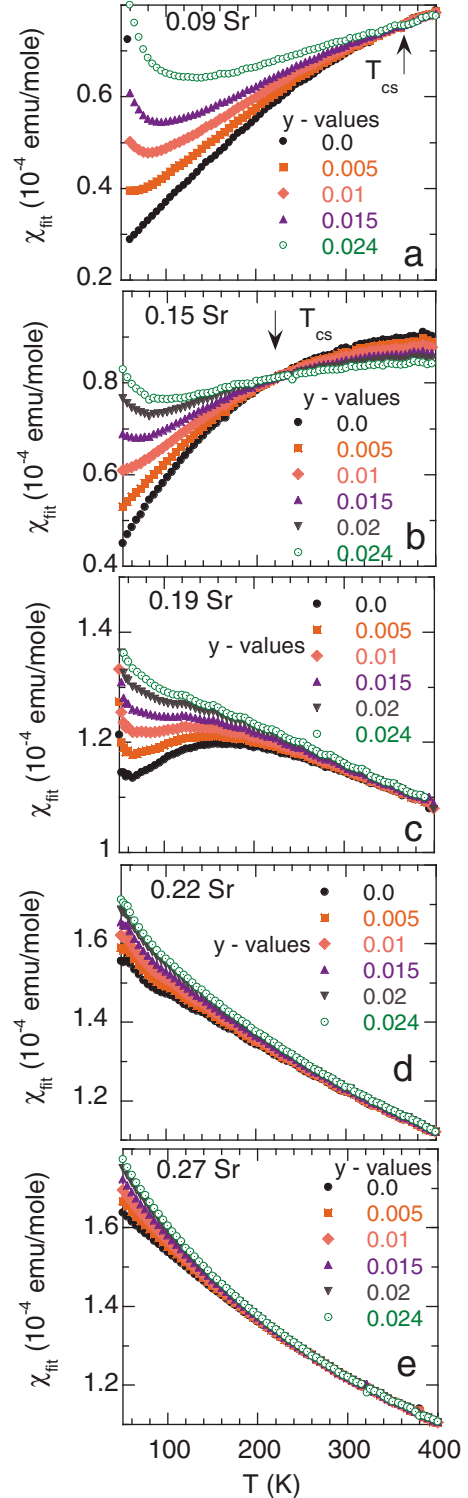


FIG. 3. (Color online) Plots of the fitted magnetic susceptibility, $\chi_{fit}(T) \equiv a_0 + a_1 y$, of $\text{La}_{2-x}\text{Sr}_x\text{Cu}_{1-y}\text{Zn}_y\text{O}_4$ compounds for the Sr and Zn contents (y) shown. The crossing temperature (see text for details) T_{cs} is marked in (a) and (b).

A. Standard local moment analysis

When conventional localized magnetic moments with a low concentration y are introduced into a normal metal the

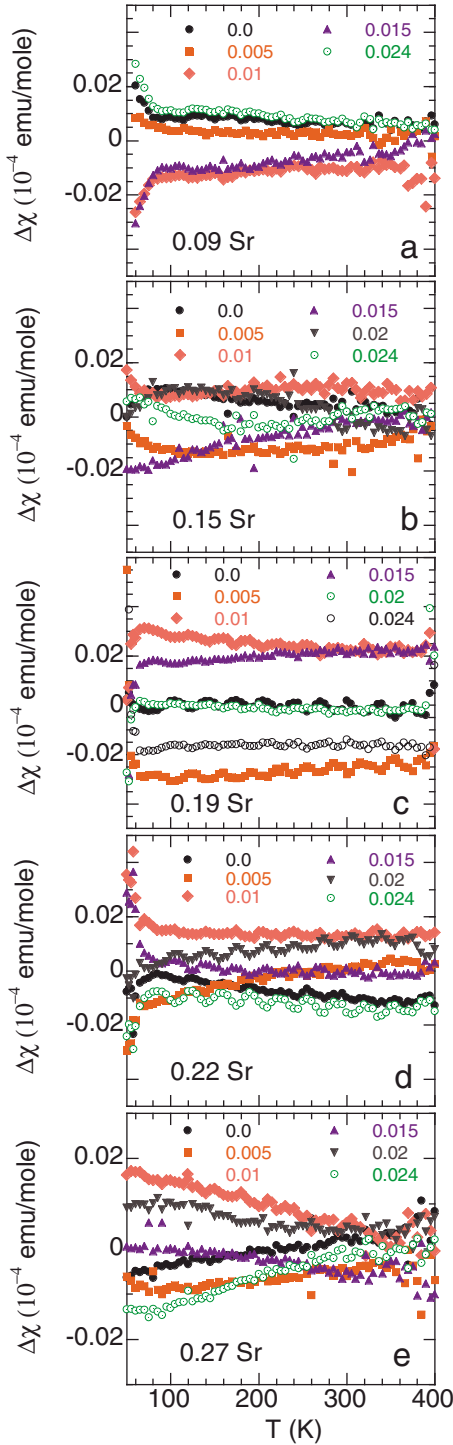


FIG. 4. (Color online) Difference plots, giving the errors $\Delta\chi = [\chi(T) - \chi_{fit}(T)]$ for $\text{La}_{2-x}\text{Sr}_x\text{Cu}_{1-y}\text{Zn}_y\text{O}_4$ compounds for the Sr (x) and Zn (y) contents are shown.

contribution to the susceptibility can usually be expressed as the sum of two independent contributions,

$$\Delta\chi(y, T)/y \equiv a_1 = C/(T + \theta) + \Delta\chi_0, \quad (2)$$

where the CW term $C/(T + \theta)$ is the response of the local magnetic moments and the dilution term $\Delta\chi_0$ expresses any change in the host susceptibility χ_0 . The Curie temperature θ

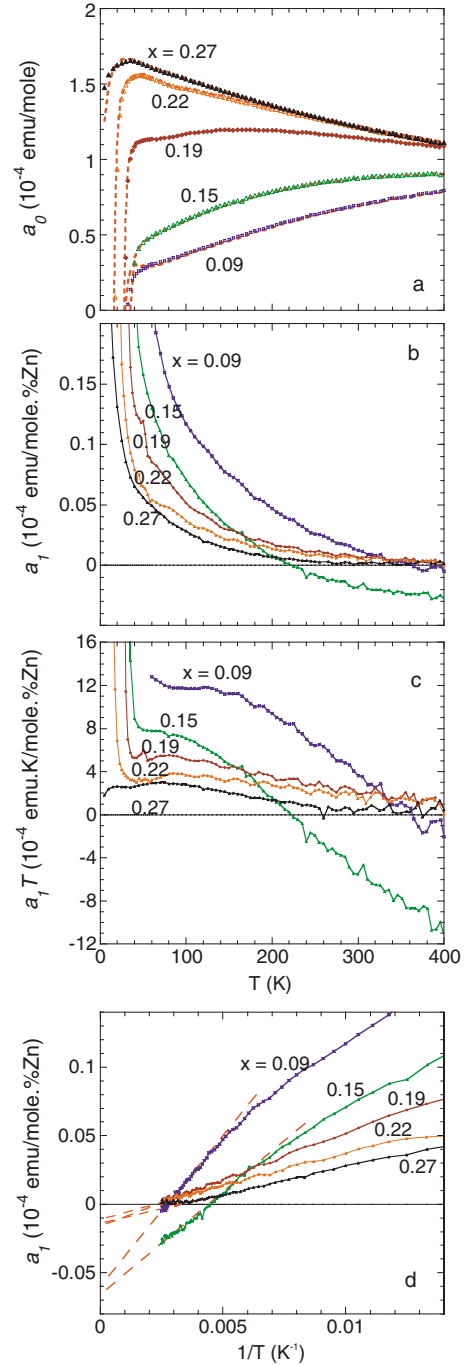


FIG. 5. (Color online) (a) Fitted values $a_0(T)$ (dotted line) and raw data for the Zn-free samples for all $\text{La}_{2-x}\text{Sr}_x\text{Cu}_{1-y}\text{Zn}_y\text{O}_4$ compounds studied. The Sr contents (x) are given in the figure. (b) The susceptibility increment $a_1(T)$ per % Zn. (c) Plots of $a_1(T)T$ for all $\text{La}_{2-x}\text{Sr}_x\text{Cu}_{1-y}\text{Zn}_y\text{O}_4$ compounds. (d) Plots of $a_1(T)$ vs $1/T$ for all $\text{La}_{2-x}\text{Sr}_x\text{Cu}_{1-y}\text{Zn}_y\text{O}_4$ compounds. Dashed lines show fits used to obtain the slopes (C_{HT}) and intercepts $\Delta\chi_{0,HT}$ at $1/T=0$ shown in Fig. 6.

reflects the characteristic energy of the magnetic excitations due, for example, to a Kondo effect, direct exchange, or Ruderman-Kittel-Kasuya-Yosida (RKKY) interactions. In normal-metal hosts $\Delta\chi_0$ is usually taken to be T independent, but we cannot assume this to be the case in the present cor-

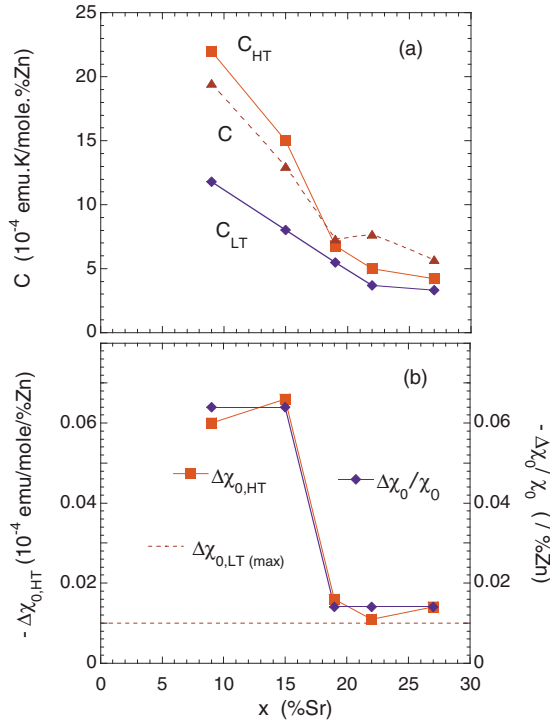


FIG. 6. (Color online) (a) Low- and high-temperature estimates of the Curie constants C_{LT} and C_{HT} obtained from Figs. 5(c) and 5(d), respectively, and values of C obtained from fits to Eq. (2), assuming that $\Delta\chi_0$ scales with χ_0 at all T , are all plotted vs Sr content x . (b) Left-hand scale $\Delta\chi_{0,HT}$ obtained from Fig. 5(d) and the upper limit to $\Delta\chi_{0,LT}$ obtained from Fig. 5(c) are plotted vs x . Right-hand scale $-\Delta\chi_0/\chi_0$ values, obtained from fits to Eq. (2), assuming that $\Delta\chi_0$ scales with χ_0 , are plotted vs x .

related materials with strongly T -dependent host susceptibilities. In this case, as discussed below, one possible assumption is that $\Delta\chi_0$ scales with, and has the same T dependence as, the host susceptibility χ_0 .

To compare our data at high temperatures with Eq. (2) we plot $a_1(T)$ versus $1/T$ in Fig. 5(d). It is immediately obvious from this figure that the intercept $\Delta\chi_{0,HT}$ as $1/T \rightarrow 0$ is large and negative for the two UD samples, with $a_1(T)$ crossing over to positive values at $T_{cs} \sim 360$ K for $x=0.09$ and 220 K for $x=0.15$ (in each case $T_{cs} \sim 80\%$ of the characteristic pseudogap temperature T^*). For the more heavily doped samples with $x=0.19, 0.22$, and 0.27 , which do not exhibit a pseudogap, the intercept $\Delta\chi_{0,HT}$ is small and Fig. 5(c) shows that there is no crossing point below 400 K. Values of the high- T Curie constant C_{HT} , and dilution term $\Delta\chi_{0,HT}$, determined from the slope and intercept of linear fits of a_1 vs $1/T$ in the temperature region ~ 200 –400 K are shown in Figs. 6(a) and 6(b), respectively.

Information on the low- T behavior can be obtained from the plot of $a_1(T)T$ versus T shown in Fig. 5(c). In this temperature region $a_1(T)T$ is relatively constant with no obvious linear term that could be attributed to $\Delta\chi_0 T$ with a constant $\Delta\chi_0$. Thus, as shown in Fig. 6(b), the dilution term $\Delta\chi_{0,LT}$ is small in this low- T range, and for the UD samples it is less than 20% of its high-temperature value $\Delta\chi_{0,HT}$. Also, according to Eq. (2), $a_1(T)T$ should fall toward zero as T falls below θ . The experimental decrease is at most very weak, so

θ must be substantially smaller than 40 K (our low- T cutoff due to the onset of superconductivity). Better estimates of θ can be obtained for the more heavily Zn-doped samples with low or zero T_c by subtracting from χ a linear extrapolation of the Zn-free susceptibility from above T_c to $T=0$ K. This yields values of $\theta \sim 15 \pm 5$ K for the UD samples. For the OD samples, the smaller CW term, uncertainties in the extrapolation of the Zn-free susceptibility, sensitivity to errors in Sr content, and the presence of SC fluctuations even for heavy Zn doping preclude a reliable estimate of θ , although the data in Fig. 5(c) do not suggest any substantial increase in θ at higher doping. The Curie constants C_{LT} given by the approximately constant values of $a_1 T$ in the low- T region are shown in Fig. 6(a). C_{LT} decreases strongly up to 19% Sr but show little change at higher doping. From C_{LT} we obtain effective magnetic moments $p_{eff} = 0.98\mu_B, 0.80\mu_B, 0.67\mu_B, 0.54\mu_B$, and $0.49\mu_B$ per Zn, for $x=0.09, 0.15, 0.19, 0.22$, and 0.27 respectively, consistent with values found in earlier studies on LSCO and yttrium barium copper oxide (Y123).^{3,18–20} The low values of θ are consistent with previous work on Zn and Li impurities in UD Y123,^{19,22} although an increase in θ has been reported for OD Y123.²²

Since it is clear that the dilution term is strongly T dependent, at least for the UD samples, we have also fitted the data above T_c to Eq. (2) on the assumption that $\Delta\chi_0$ scales with χ_0 . (Actually there are systematic deviations at high temperatures indicating that $\Delta\chi_0$ and χ_0 may in fact have rather different T dependences.) Since the low values of θ are poorly determined from fits above 60 K, we kept $\theta=15$ K in each case. The fitted values of C and $\Delta\chi_0/\chi_0$ are shown in Figs. 6(a) and 6(b), respectively. Values for the Curie constant C are substantially higher than C_{LT} , but are comparable with the values C_{HT} , dropping sharply to $x=0.19$ and then remaining essentially constant at higher x . The dilution term $\Delta\chi_0/\chi_0$ drops even more sharply from $\sim 0.064/\%$ Zn for $x=0.09$ and 0.15 , to $0.014/\%$ Zn for $x \geq 0.19$. For $x \geq 0.19$ it is therefore reasonable to ascribe $\Delta\chi_0$ to a dilution effect. However, for the two underdoped samples, $\Delta\chi_0$ is far too large to be interpreted in this way and suggests a more dramatic redistribution of spin spectral weight.

We conclude that fitting our data to Eq. (2) leads, for the UD samples, to values of the Curie constant C and the dilution term $\Delta\chi_0$ that depend strongly on the temperature region of the fit. This suggests that the simple local moment behavior described by Eq. (2) is inadequate to explain the susceptibility of these samples

B. Model-independent analysis

A revealing presentation of the data which provides model-independent information on the energy distribution of the spin excitations is given by plots of a_0^* and a_1^* vs T shown in Fig. 7. We define $\chi^* = d(\chi T)/dT$, with corresponding expressions a_0^* and a_1^* for the susceptibility components a_0 and a_1 . While $\chi(T)$ is sensitive to all spin excitations in a thermal energy window extending from zero to $\sim 3k_B T - 4k_B T$, it can be shown that χ^* reflects the number in a narrower energy region $\sim 2k_B T \pm k_B T$. This is a general result which does not depend on the nature of the spin excitations or their statistics,

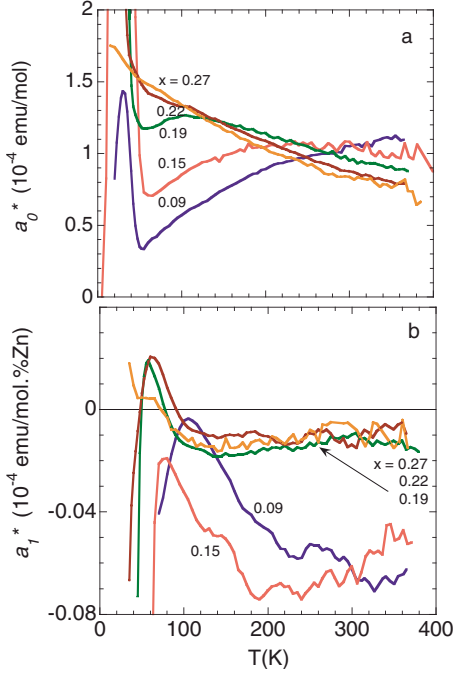


FIG. 7. (Color online) (a) $a_0^* = d(a_0 T)/dT$ for the Zn-free material (smoothed over seven data points) and (b) $a_1^* = d(a_1 T)/dT$ for the increment per % Zn (smoothed over 13 data points). These plots narrow the Curie-Weiss term and show more clearly changes in the DOS at higher temperature.

e.g., Fermi-Dirac, Bose-Einstein, or classical. Hence χ^* excludes the zero- and low-energy excitations that may dominate $\chi(T)$ at all temperatures and provides a sharper representation of the DOS of the spin excitation spectrum. For example, the Curie-Weiss term $\chi = C/(T + \theta)$ which dominates the present susceptibility data over almost the entire T range becomes a much narrower function $\chi^* = C\theta/(T + \theta)^2$, which more closely reflects the energy range $\sim k_B \theta$ of the underlying excitations. Note that $\chi^* = 0$ for a pure Curie term $\chi = C/T$, and $\chi^* = \chi$ if χ is T independent.

Plots of $a_0^*(T)$ for the Zn-free material in Fig. 7(a) clearly show that the pseudogap falls with increasing p and is absent for $x > 19\%$ Sr. Figure 7(b) shows that the increment a_1^* per % Zn is strikingly different above and below 19% Sr. For the 19%, 22%, and 27% Sr samples, a_1^* is small, negative, and only weakly T dependent, with magnitude similar to the values of $\Delta\chi_{0,HT}$ shown in Fig. 6(b). By contrast, for the 9% and 15% Sr samples, a_1^* exhibits large and broad minima at temperatures of ~ 400 and 230 K, respectively, comparable with the peak temperatures in a_0^* (see Fig. 7). These broad negative regions clearly account for the large negative high-temperature dilution terms $\Delta\chi_{0,HT}$ for the UD samples shown in Fig. 6(b) when the data are expressed in terms of Eq. (2).

In Fig. 7(b) we see only the “tails” of low- T upturns in $a_1^*(T)$ because of the dominance of SC correlations below 60 K and the low value $\theta \sim 15$ K. (Recall that a_1^* is not affected by a pure Curie term with $\theta = 0$ K.) However, we can determine a_1^* at lower temperatures for heavily Zn-doped samples with low or zero T_c from $a_1^* \sim [\chi^*(y, T) - \chi_{extrap}^*(0, T)]/y$ where $\chi_{extrap}^*(0, T)$ is a linear extrapolation of the Zn-free data from above T_c to $T = 0$ K. As shown in Fig. 8 a clear

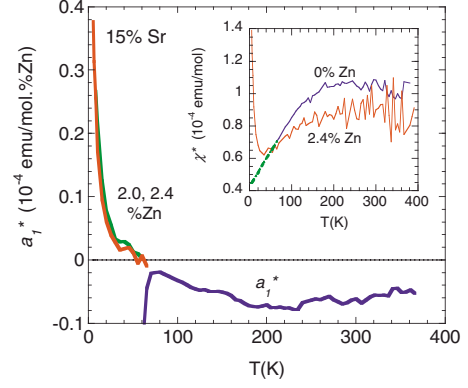


FIG. 8. (Color online) Main figure: $a_1^* \text{ vs } T$ for 15% Sr. Above 60 K the curve is derived from a linear fit for all Zn contents [shown in Fig. 7(b)]. Below 60 K data for weakly or nonsuperconducting 2.0% and 2.4% Zn samples assuming a linear extrapolation of the Zn-free normal state χ^* to below T_c (see text). Inset: $\chi^* = d(\chi T)/dT$ for 15% Sr containing 0% and 2.4% Zn. The figure suggests that the low-temperature peak in Zn-doped samples results from the softening of higher-energy states in the Zn-free samples.

upturn is then visible for the 15% Sr sample containing 2.0% and 2.4% Zn. The upturn per % Zn below 60 K is independent of y , confirming the absence of SC correlations for these higher Zn levels. A fit of a_1^* to $C\theta/(T + \theta)^2$ for these two samples yields $\theta \sim 8$ K and C close to the value C_{LT} shown in Fig. 6.

The positive low- T upturn in the main part of Fig. 8, together with the negative area under the a_1^* curve at higher temperatures, suggests that the low-energy states are formed at the expense of spectral weight from higher energies in the normal-state spectrum. This is also demonstrated in the inset to Fig. 8, where we show χ^* for 15% Sr containing 0% Zn (with a linear extrapolation below 60 K) and raw χ^* data for 2.4% Zn. It is evident from this plot that weight is lost in the normal-state spectrum predominantly from the region of the peak in χ^* for the Zn-free material, i.e., from the shoulder region of the pseudogap.

For the 9% Sr sample a fit of the low-temperature upturn to $C\theta/(T + \theta)^2$ gives $\theta \sim 14$ K and C around 25% higher than C_{LT} . Inspection of the a_1^* and a_0^* data in Figs. 7(a) and 7(b) suggests that for the 9% Sr sample also, Zn doping transfers spectral weight to low energies from the shoulder region of the pseudogap.

C. Comparison with other interpretations

If we accept this circumstantial evidence that the low-energy states induced by Zn doping are derived from higher-energy states in the normal-state spectrum of the Zn-free host, then clearly these states must have similar character (i.e., both are spins or both are quasiparticles). The strongly temperature- and doping-dependent susceptibility of pure LSCO [Figs. 1 and 5(a)] was originally attributed²¹ to short-range antiferromagnetic correlations of the Cu spins. Here, the broad susceptibility maxima at temperatures T_{peak} that decrease with hole doping reflect the mean energy ($\sim k_B T_{peak}$) of the short-range spin correlations. For localized

Cu spins, it is a clear prediction of the short-range AF order scenario that the magnitude of the susceptibility peak $\chi(T_{peak}) \propto 1/T_{peak}$, since the number of Cu spins is doping independent. As noted in Ref. 21 [see also Fig. 5(a)] this is not observed and was provisionally ascribed²¹ to a decrease in the effective moment per Cu by a factor of 5 between $x=0.0$ and 0.2. However the entropy, which empirically¹⁷ corresponds to the quantity χT , is linked to the number of available states, rather than to the size of the effective moment. So in our view the serious discrepancy regarding $\chi(T_{peak})$ and $1/T_{peak}$ casts doubt on the suggestion that the pseudogap in the pure material is a spin gap associated with short-range antiferromagnetic interactions between localized spins. Instead the close correspondence¹⁷ between the susceptibility and the electronic specific heat or entropy ($\chi \sim R_0 S/T$, where S is the electronic entropy and R_0 is the free electron Wilson ratio) suggests that both quantities (χ and S/T) are dominated by the QP spectrum. Their T dependences reflect the energy dependence due to the pseudogap in the QP DOS, and a value of R_0 close to its free electron value simply implies that spin and charge excitations make a comparable contribution to the entropy. *This does not mean that electron correlations are weak—only that the low-energy excitations resemble those of a system of fermions.* The conclusion that the pseudogap exists in the QP DOS and is not simply a spin gap has been confirmed by angle-resolved photo-emission spectroscopy data for LSCO (Ref. 23) as well as other cuprates.

Our experiments have demonstrated that in UD samples the introduction of nonmagnetic Zn ions introduces additional low-energy excitations with energy $k_B\theta \sim 15$ K giving a Curie-like magnetic response and, in addition, causes a strong depletion of spin spectral weight in the energy region $k_B T^*$ characteristic of the pseudogap. For more heavily doped samples with $x \geq 0.19$, in which the pseudogap is absent, the Curie term is strongly reduced and there is little loss of spectral weight at higher energies. There are several possible interpretations of these results.

(i) The Curie-like term is a spin-only effect associated with the local magnetism of neighboring Cu spins around the nonmagnetic Zn impurity. This is the conclusion drawn from the staggered magnetic response observed in NMR studies.^{7,22} This is an attractive option since the increase in the magnetic correlation length with underdoping would explain the corresponding progressive increase in Zn-induced Curie constant (Fig. 6). It is, however, hard to understand why the characteristic energy of the Cu spins neighboring the Zn impurity ($\theta \sim 15$ K) should be a factor 20–30 lower than the interaction energies of more distant Cu spins ($T_{peak} \sim 300$ –500 K). It would also not explain the strong loss of spectral weight around the pseudogap energy or the *very abrupt* reduction in the induced moment when the pseudogap closes. Therefore, from our point of view, the Curie law observed in the T dependence of the ⁸⁹Y nearest-neighbor NMR line in $YBa_2(Cu_{1-y}Zn_y)_3O_{6.64}$ (Ref. 7) arises from the low-energy structure in the quasiparticle DOS rather than from magnetic moments, localized at or near the Zn sites.

(ii) The Curie-like term is due to a Kondo resonance ($T_K \sim 15$ K) located within the complex of the Zn ion and its neighboring Cu spins.²² This is also a strong candidate as it would explain the loss of weight from the host conduction

band at rather higher energies. It would however be necessary to explain why it is so sensitive to the presence of a pseudogap and is so strongly reduced when the pseudogap closes, and also, how does such a narrow resonance ($T_K \sim 15$ K) survive in UD samples in the presence of very much stronger Cu-Cu exchange energies ($T_{peak} \sim 300$ –500 K).

(iii) The Curie-like term is due to a narrow quasiparticle resonance close to the Fermi energy, induced by unitary scattering from the Zn ion. This is analogous to the QP resonances on Zn ions observed within the superconducting gap of $Bi_2Sr_2CaCu_2O_{8+\delta}$ by scanning tunneling microscopy,¹¹ whose energy and spatial dependence have been calculated successfully.²⁴ It is also predicted²⁵ to occur whenever there is a very low DOS caused by the pseudogap. In this interpretation the observed energy width of the resonance (here, we find $k_B\theta \sim 15$ K) would be close to the width of resonances calculated (~ 20 K) (Ref. 24) and observed (half width at half maximum of ~ 20 K)¹¹ inside the superconducting gap. The resonance is also expected to be drawn predominantly from states at the edge of the pseudogap, e.g., as shown by the calculations for a d -density-wave pseudogap in Ref. 26, in agreement with our observations. This interpretation readily explains (a) the large Curie term in Zn-doped samples with a pseudogap, accompanied by a substantial suppression of spectral weight at higher energies; (b) the abrupt decrease in C as the pseudogap closes at 19% Sr; (c) the rather weak effect of Zn doping on the susceptibility of more heavily doped samples where the pseudogap is absent; and (d) the approximate magnitude of the Curie temperature θ .

Our bulk susceptibility results only refer to the uniform ($Q=0$) static ($\omega=0$) part of the generalized susceptibility $\chi(Q, \omega)$. As documented in a recent review paper,²⁷ important information about the spatial dependence of the magnetic response has been obtained by NMR measurements and on the Q dependence from neutron studies, for a variety of impurity-substituted cuprates. We believe that our results, on the energy distribution of the spin spectral weight induced by Zn doping of this correlated-electron system, complement these other studies of the spatial dependence. Our work suggests that the spin and charge degrees of freedom seem to be inextricably mixed in the cuprates and point toward an important energy dependence of the DOS.

V. CONCLUSIONS

In summary, we have studied the static magnetic susceptibility of $La_{2-x}Sr_xCu_{1-y}Zn_yO_4$ over a wide range of hole concentration and Zn contents. Nonmagnetic Zn doping is found to induce a Curie-Weiss term in the susceptibility, which is large in underdoped materials with a pseudogap ($x < 0.19$) but is rather small and doping independent in more heavily doped materials where the pseudogap is absent.^{28–30} Similar results were found for Zn-doped Y123.^{19,22}

A model-independent analysis of our data has shown that in samples with a pseudogap the additional low-energy excitations giving rise to the Curie-Weiss term are accompanied by a strong reduction in spin spectral weight in the shoulder

region of the pseudogap. This effect vanishes abruptly when the pseudogap closes and is absent in more heavily doped samples. We have considered several interpretations of these results, and we conclude that a quasiparticle resonance deep in the pseudogap, induced by unitary scattering by the Zn ions, would account for our observations. Nevertheless, we accept that in these very strongly correlated materials, the remarkable effects associated with Zn doping may have a deeper origin.

ACKNOWLEDGMENTS

We thank J. L. Tallon for helpful comments and suggestions. S.H.N. acknowledges financial support from the Commonwealth Scholarship Commission (U.K.) and the Department of Physics, Cambridge University. R.S.I. acknowledges financial support from Trinity College, Cambridge and the Cambridge Commonwealth Trust (U.K.). All experimental work in Cambridge was supported by the EPSRC (U.K.).

*Corresponding author; salehnaqib@yahoo.com

- ¹J. M. Tarascon, L. H. Greene, P. Barboux, W. R. Mckinnon, G. W. Hull, T. P. Orlando, K. A. Delin, S. Foner, and E. J. McNiff, Jr., *Phys. Rev. B* **36**, 8393 (1987).
- ²T. R. Chien, Z. Z. Whang, and N. P. Ong, *Phys. Rev. Lett.* **67**, 2088 (1991).
- ³S. Zagoulaev, P. Monod, and J. Jegoudez, *Phys. Rev. B* **52**, 10474 (1995).
- ⁴J. L. Tallon, J. R. Cooper, P. S. I. P. N. de Silva, G. V. M. Williams, and J. W. Loram, *Phys. Rev. Lett.* **75**, 4114 (1995).
- ⁵A. M. Finkel'stein, V. E. Kataev, E. F. Kukovitskii, and G. B. Teitel'baum, *Physica C* **168**, 370 (1990).
- ⁶H. Alloul, P. Mendels, H. Casalta, J. F. Marucco, and J. Arabski, *Phys. Rev. Lett.* **67**, 3140 (1991).
- ⁷A. V. Mahajan, H. Alloul, G. Collin, and J. F. Marucco, *Phys. Rev. Lett.* **72**, 3100 (1994).
- ⁸S. Zagoulaev, P. Monod, and J. Jegoudez, *Physica C* **259**, 271 (1996).
- ⁹G. Xiao, M. S. Cieplak, J. Q. Xiao, and C. L. Chien, *Phys. Rev. B* **42**, 8752 (1990).
- ¹⁰N. Ishikawa, N. Kuroda, H. Ikeda, and R. Yoshizaki, *Physica C* **203**, 284 (1992).
- ¹¹S. H. Pan, E. W. Hudson, K. M. Lang, H. Eisaki, S. Uchida, and J. C. Davis, *Nature (London)* **403**, 746 (2000).
- ¹²J. W. Loram, K. A. Mirza, J. M. Wade, J. R. Cooper, and W. Y. Liang, *Physica C* **235-240**, 134 (1994).
- ¹³J. R. Cooper and J. W. Loram, *J. Phys. I* **6**, 2237 (1996).
- ¹⁴H. F. Fong, P. Bourges, Y. Sidis, L. P. Regnault, J. Bossy, A. Ivanov, D. L. Milius, I. A. Aksay, and B. Keimer, *Phys. Rev. Lett.* **82**, 1939 (1999).
- ¹⁵R. S. Islam, Ph.D. thesis, University of Cambridge, 2005.
- ¹⁶See supplementary material at <http://link.aps.org/supplemental/10.1103/PhysRevB.81.054511> for the susceptibility data (measured at 5 T) shown in Fig. 1.
- ¹⁷J. W. Loram, J. Luo, J. R. Cooper, W. Y. Liang, and J. L. Tallon, *J. Phys. Chem. Solids* **62**, 59 (2001).
- ¹⁸R. S. Islam, J. R. Cooper, J. W. Loram, and S. H. Naqib, *Physica C* **460-462**, 753 (2007).
- ¹⁹P. Mendels, J. Bobroff, G. Collin, H. Alloul, M. Gabay, J. F. Marucco, N. Blanchard, and B. Grenier, *EPL* **46**, 678 (1999).
- ²⁰T. Nakano, M. Oda, C. Manabe, N. Momono, Y. Miura, and M. Ido, *Phys. Rev. B* **49**, 16000 (1994).
- ²¹D. C. Johnston, *Phys. Rev. Lett.* **62**, 957 (1989).
- ²²J. Bobroff, W. A. MacFarlane, H. Alloul, P. Mendels, N. Blanchard, G. Collin, and J.-F. Marucco, *Phys. Rev. Lett.* **83**, 4381 (1999).
- ²³A. Ino, C. Kim, M. Nakamura, T. Yoshida, T. Mizokawa, A. Fujimori, Z.-X. Shen, T. Kakeshita, H. Eisaki, and S. Uchida, *Phys. Rev. B* **65**, 094504 (2002).
- ²⁴I. Martin, A. V. Balatsky, and J. Zaanen, *Phys. Rev. Lett.* **88**, 097003 (2002).
- ²⁵H. V. Kruis, I. Martin, and A. V. Balatsky, *Phys. Rev. B* **64**, 054501 (2001).
- ²⁶A. V. Balatsky, I. Vekhter, and J.-X. Zhu, *Rev. Mod. Phys.* **78**, 373 (2006).
- ²⁷H. Alloul, J. Bobroff, M. Gabay, and P. J. Hirschfeld, *Rev. Mod. Phys.* **81**, 45 (2009).
- ²⁸S. H. Naqib, J. R. Cooper, J. L. Tallon, R. S. Islam, and R. A. Chakalov, *Phys. Rev. B* **71**, 054502 (2005).
- ²⁹S. H. Naqib, J. R. Cooper, J. L. Tallon, and C. Panagopoulos, *Physica C* **387**, 365 (2003).
- ³⁰J. L. Tallon and J. W. Loram, *Physica C* **349**, 53 (2001).